The prognosis of HCC patients stratified by the EOB-AFP classification was most likely affected by the malignant nature of the tumor at surgical resection, because EOB-AFP class C patients showed a 40-60% recurrence-free survival rate, whereas class A patients had a 88-100% recurrence-free survival rate at 1 year after radical resection in both cohorts (Fig. S5).

Altogether, our data, for the first time, revealed that the prognosis of early-stage HCC patients is heterogeneous and related to the malignant phenotypes of the tumors, even after successful treatment by radical resection. The EOB-AFP classification system reflects the malignant nature of the tumor and predicts the survival of early-stage HCC patients prior to surgery.

Discussion

Among several HCC staging systems currently used,[2] the BCLC system is recommended because it is linked to treatment strategy.[22] The assessment of the malignant nature of tumors coupled with current staging systems will supplement the management of early-stage HCC[23] because early recurrence after potentially curative treatment may be associated with the characteristics of the resected tumor rather than the development of a *de novo* HCC in the background liver.[24] Molecular profiling approaches have tried to evaluate the malignant features of HCCs and the surrounding noncancerous liver tissue,[3-6,12,18] although the evaluation of the potential clinical application of these approaches is ongoing. Our EOB-AFP classification system is molecularly related to the *OATP1B3* gene signature, which can be used to classify HCCs according to their stem/maturational status. Interestingly, the differential expression of *OATP1B3* was also noted in two HCC subtypes associated with the stem/maturational status, as reported recently by our group (hepatic stem cell-like and mature hepatocyte-like HCC)[12] and others (hepatoblast-type and hepatocyte type)[4] (Fig. S6). As expected, all class A HCCs were categorized as mature hepatocyte-like HCC in Cohort 1 (data not shown). The stem/maturational status defined by the EOB-AFP classification is most likely regulated by at least two transcription factors: HNF4α and FOXM1 (Fig. 4E).

HNF4α was first discovered as a liver-enriched nuclear orphan receptor activating the transcription of transthyretin genes, and it is known to regulate bile acid and cholesterol metabolism.[25] The liver-specific loss of *HNF4A* in adult mice results in hepatocyte proliferation,[26] whereas the introduction of *HNF4A* suppresses HCC growth.[27,28] Furthermore, a recent study suggested a role for *HNF4A* as a tumor suppressor in inflammation-related hepatocarcinogenesis through the regulation of microRNAs.[29] The present study demonstrated a crucial role for HNF4α in maintaining a hepatocyte-like, less aggressive phenotype coupled with Gd-EOB-DTPA uptake in a class A HCC by directly modifying *HNF4A* gene expression. Thus, *HNF4A* may work as a tumor suppressor gene and inhibit the progression of HCC, which may be related to the good prognosis of class A HCCs.

FOXM1 belongs to the forkhead superfamily of transcription factors and regulates a myriad of biologic processes including cell proliferation and differentiation.[30] The pivotal role of FOXM1 in liver development and regeneration has been reported previously.[17] FOXM1 was also required for HCC development in a mouse hepatocarcinogenesis model[31] and acted as an oncogene in a transgenic mouse model.[32] It was recently shown that FOXM1 levels are elevated in various cancers including HCC.[32,33] A prognostic role for FOXM1 in HCC patients after liver transplantation was also reported[34]; this may be associated with the metastatic capacity of tumors regulated by FOXM1.[35] As FOXM1 and AFP are known to be activated during liver regeneration and hepatocarcinogenesis, serum AFP levels may be a surrogate marker for the expression status of FOXM1 and thus facilitate the prognostic stratification of HCCs by the EOB-AFP classification.

Among the molecular markers reported to be differentially expressed between dysplastic nodule and well-differentiated HCC, we found preferential overexpression of GS in EOB-AFP class A and GPC-3 in class C HCCs. Our data suggest that class A and class C HCCs may follow different processes of early hepatocarcinogenesis events that might be associated with the differential activation of HNF4α and FOXM1, and further studies are required to obtain molecular insights into these processes.

Our overall survival data in Cohort 2 indicated that EOB-AFP class A patients had 100% overall survival, whereas class C patients had 30% overall survival at 1,200 days after radical resection. This suggests that the micro-dissemination of tumor cells in EOB-AFP class C HCC patients has already occurred by the time they are diagnosed with early-stage disease. Indeed, 50% of all class C patients showed tumor recurrence, whereas 88-100% of class A patients showed no recurrence within 1 year of resection; this is consistent with a recent study evaluating the clinical features of hyperintense HCCs[36] and may be due to

the overexpression of FOXM1, which results in the activation of metastatic programs. Therefore, these patients might have survival benefits if they receive adjuvant therapies. As several adjuvant therapies might be beneficial for HCC patients after surgical resection,[37] integration of the EOB-AFP classification system into current staging practices may provide additional therapeutic options for early-stage HCC patients who will receive surgery.

A limitation of the present study is that we used three different cohorts to reveal the molecular portraits associated with clinical imaging and prognosis (i.e., the microarray cohort of 238 HCCs of various stages for the evaluation of molecular profiling; Cohort 1 for the validation of molecular profiling and EOB-MRI findings in various stages of HCC; and Cohort 2 for evaluating the utility of EOB-MRI and serum AFP in predicting the prognosis of early-stage HCCs), which made the molecular and prognostic analyses complex. Another limitation of this study was in the evaluation of prognostic utility because it uses small retrospective cohorts. Direct evaluation of the molecular profiles and prognostic values of hyperintense HCCs should be performed in a prospective study using a large-scale HCC cohort.

Taken together, the present study demonstrates for the first time that the combined approach of noninvasive Gd-EOB-DTPA-enhanced MRI and serum AFP levels can be used preoperatively to classify resectable HCCs into three subgroups with distinct prognoses. This classification is molecularly related to the stem/maturation status of HCCs regulated by HNF4α and FOXM1. The multicenter early-stage HCC cohort that received radical resection revealed that the EOB-AFP classification is clinically useful to determine the prognosis of early-stage HCC patients. On the basis of these observations, we propose that the EOB-AFP classification system be incorporated into current HCC staging practices, especially for the management of early-stage HCCs.

Acknowledgment: We thank Drs. Yutaka Aoyagi (Division of Gastroenterology and Hepatology, Niigata University Graduate School of Medical and Dental Sciences, Niigata, Japan), Hiroko Iijima (Division of Hepatobiliary and Pancreatic Disease, Department of Internal Medicine, Hyogo College of Medicine, Hyogo, Japan), and Michio Sata (Division of Gastroenterology, Department of Medicine, Kurume University School of Medicine, Kurume, Japan) for help with patient enrollment. We also thank Mss. Masayo Baba and Nami Nishiyama for excellent technical assistance.

References

1. Jemal A, Bray F, Center MM, Ferlay J, Ward E, Forman D. Global cancer statistics. CA Cancer J Clin 2011;61:69-90.
2. Sala M, Forner A, Varela M, Bruix J. Prognostic prediction in patients with hepatocellular carcinoma. Semin Liver Dis 2005;25:171-180.
3. Cairo S, Wang Y, de Reynies A, Duroure K, Dahan J, Redon MJ, et al. Stem cell-like micro-RNA signature driven by Myc in aggressive liver cancer. Proc Natl Acad Sci U S A 2010;107:20471-20476.
4. Lee JS, Heo J, Libbrecht L, Chu IS, Kaposi-Novak P, Calvisi DF, et al. A novel prognostic subtype of human hepatocellular carcinoma derived from hepatic progenitor cells. Nat Med 2006;12:410-416.
5. Marquardt JU, Raggi C, Andersen JB, Seo D, Avital I, Geller D, et al. Human hepatic cancer stem cells are characterized by common stemness traits and diverse oncogenic pathways. HEPATOLOGY 2011;54:1031-1042.
6. Yamashita T, Ji J, Budhu A, Forgues M, Yang W, Wang HY, et al. EpCAM-positive hepatocellular carcinoma cells are tumor-initiating cells with stem/progenitor cell features. Gastroenterology 2009;136:1012-1024.
7. Yamashita T, Wang XW. Cancer stem cells in the development of liver cancer. J Clin Invest 2013;123:1911-1918.
8. Reimer P, Schneider G, Schima W. Hepatobiliary contrast agents for contrast-enhanced MRI of the liver: properties, clinical development and applications. Eur Radiol 2004;14:559-578.
9. Kanki A, Tamada T, Higaki A, Noda Y, Tanimoto D, Sato T, et al. Hepatic parenchymal enhancement at Gd-EOB-DTPA-enhanced MR imaging: correlation with morphological grading of severity in cirrhosis and chronic hepatitis. Magn Reson Imaging 2012;30:356-360.
10. Kitao A, Matsui O, Yoneda N, Kozaka K, Shinmura R, Koda W, et al. The uptake transporter OATP8 expression decreases during multistep hepatocarcinogenesis: correlation with gadoxetic acid enhanced MR imaging. Eur Radiol 2011;21:2056-2066.
11. Kitao A, Zen Y, Matsui O, Gabata T, Kobayashi S, Koda W, et al. Hepatocellular carcinoma: signal intensity at gadoxetic acid-enhanced MR Imaging—correlation with molecular transporters and histopathologic features. Radiology 2010;256:817-826.
12. Yamashita T, Forgues M, Wang W, Kim JW, Ye Q, Jia H, et al. EpCAM and alpha-fetoprotein expression defines novel prognostic subtypes of hepatocellular carcinoma. Cancer Res 2008;68:1451-1461.
13. Yamashita T, Honda M, Nakamoto Y, Baba M, Nio K, Hara Y, et al. Discrete nature of EpCAM(+) and CD90(+) cancer stem cells in human hepatocellular carcinoma. HEPATOLOGY 2013;57:1484-1497.
14. Yamashita T, Honda M, Nio K, Nakamoto Y, Takamura H, Tani T, et al. Oncostatin m renders epithelial cell adhesion molecule-positive liver cancer stem cells sensitive to 5-Fluorouracil by inducing hepatocytic differentiation. Cancer Res 2010;70:4687-4697.
15. Lade AG, Monga SP. Beta-catenin signaling in hepatic development and progenitors: which way does the WNT blow? Dev Dyn 2011;240:486-500.
16. Trauner M, Halilbasic E. Nuclear receptors as new perspective for the management of liver diseases. Gastroenterology 2011;140:1120-1125 e1121-1112.
17. Wang X, Kiyokawa H, Dennewitz MB, Costa RH. The Forkhead Box m1b transcription factor is essential for hepatocyte DNA replication and mitosis during mouse liver regeneration. Proc Natl Acad Sci U S A 2002;99:16881-16886.
18. Hoshida Y, Villanueva A, Kobayashi M, Peix J, Chiang DY, Camargo A, et al. Gene expression in fixed tissues and outcome in hepatocellular carcinoma. N Engl J Med 2008;359:1995-2004.
19. Ji J, Shi J, Budhu A, Yu Z, Forgues M, Roessler S, et al. MicroRNA expression, survival, and response to interferon in liver cancer. N Engl J Med 2009;361:1437-1447.
20. Di Tommaso L, Destro A, Seok JY, Balladore E, Terracciano L, Sangiovanni A, et al. The application of markers (HSP70 GPC3 and GS) in liver biopsies is useful for detection of hepatocellular carcinoma. J Hepatol 2009;50:746-754.

21. Llovet JM, Chen Y, Wurmbach E, Roayaie S, Fiel MI, Schwartz M, et al. A molecular signature to discriminate dysplastic nodules from early hepatocellular carcinoma in HCV cirrhosis. Gastroenterology 2006;131:1758-1767.
22. Sherman M. Hepatocellular carcinoma: screening and staging. Clin Liver Dis 2011;15:323-334, vii-x.
23. Villanueva A, Hoshida Y, Toffanin S, Lachenmayer A, Alsinet C, Savic R, et al. New strategies in hepatocellular carcinoma: genomic prognostic markers. Clin Cancer Res 2010;16:4688-4694.
24. de Lope CR, Tremosini S, Forner A, Reig M, Bruix J. Management of HCC. J Hepatol 2012;56 Suppl:S75-87.
25. Crestani M, De Fabiani E, Caruso D, Mitro N, Gilardi F, Vigil Chacon AB, et al. LXR (liver X receptor) and HNF-4 (hepatocyte nuclear factor-4): key regulators in reverse cholesterol transport. Biochem Soc Trans 2004;32:92-96.
26. Bonzo JA, Ferry CH, Matsubara T, Kim JH, Gonzalez FJ. Suppression of hepatocyte proliferation by hepatocyte nuclear factor 4alpha in adult mice. J Biol Chem 2012;287:7345-7356.
27. Ning BF, Ding J, Yin C, Zhong W, Wu K, Zeng X, et al. Hepatocyte nuclear factor 4 alpha suppresses the development of hepatocellular carcinoma. Cancer Res 2010;70:7640-7651.
28. Yin C, Lin Y, Zhang X, Chen YX, Zeng X, Yue HY, et al. Differentiation therapy of hepatocellular carcinoma in mice with recombinant adenovirus carrying hepatocyte nuclear factor-4alpha gene. HEPATOLOGY 2008;48:1528-1539.
29. Hatziapostolou M, Polytarchou C, Aggelidou E, Drakaki A, Poultsides GA, Jaeger SA, et al. An HNF4alpha-miRNA inflammatory feedback circuit regulates hepatocellular oncogenesis. Cell 2011;147:1233-1247.
30. Koo CY, Muir KW, Lam EW. FOXM1: From cancer initiation to progression and treatment. Biochim Biophys Acta 2012;1819:28-37.
31. Kalinichenko VV, Major ML, Wang X, Petrovic V, Kuechle J, Yoder HM, et al. Foxm1b transcription factor is essential for development of hepatocellular carcinomas and is negatively regulated by the p19ARF tumor suppressor. Genes Dev 2004;18:830-850.
32. Kalin TV, Ustiyan V, Kalinichenko VV. Multiple faces of FoxM1 transcription factor: lessons from transgenic mouse models. Cell Cycle 2011;10:396-405.
33. Calvisi DF, Pinna F, Ladu S, Pellegrino R, Simile MM, Frau M, et al. Forkhead box M1B is a determinant of rat susceptibility to hepatocarcinogenesis and sustains ERK activity in human HCC. Gut 2009;58:679-687.
34. Sun H, Teng M, Liu J, Jin D, Wu J, Yan D, et al. FOXM1 expression predicts the prognosis in hepatocellular carcinoma patients after orthotopic liver transplantation combined with the Milan criteria. Cancer Lett 2011;306:214-222.
35. Raychaudhuri P, Park HJ. FoxM1: a master regulator of tumor metastasis. Cancer Res 2011;71:4329-4333.
36. Kitao A, Matsui O, Yoneda N, Kozaka K, Kobayashi S, Koda W, et al. Hypervascular hepatocellular carcinoma: correlation between biologic features and signal intensity on gadoxetic acid-enhanced MR images. Radiology 2012;265:780-789.
37. Zhong JF, Li H, Li LQ, You XM, Zhang Y, Zhao YN, et al. Adjuvant therapy options following curative treatment of hepatocellular carcinoma: a systematic review of randomized trials. Eur J Surg Oncol 2012;38:286-295.

Supporting Information

Additional Supporting Information may be found in the online version of this article at the publisher's website.

Cancer Immunol Immunother
DOI 10.1007/s00262-013-1514-7

ORIGINAL ARTICLE

In vivo immunological antitumor effect of OK-432-stimulated dendritic cell transfer after radiofrequency ablation

Hidetoshi Nakagawa · Eishiro Mizukoshi · Noriho Iida · Takeshi Terashima · Masaaki Kitahara · Yohei Marukawa · Kazuya Kitamura · Yasunari Nakamoto · Kazumasa Hiroishi · Michio Imawari · Shuichi Kaneko

Received: 1 June 2013 / Accepted: 17 December 2013

Abstract Radiofrequency ablation therapy (RFA) is a radical treatment for liver cancers and induces tumor antigen-specific immune responses. In the present study, we examined the antitumor effects of focal OK-432-stimulated dendritic cell (DC) transfer combined with RFA and analyzed the functional mechanisms involved using a murine model. C57BL/6 mice were injected subcutaneously with colon cancer cells (MC38) in their bilateral flanks. After the establishment of tumors, the subcutaneous tumor on one flank was treated using RFA, and then OK-432-stimulated DCs were injected locally. The antitumor effect of the treatment was evaluated by measuring the size of the tumor on the opposite flank, and the immunological responses were assessed using tumor-infiltrating lymphocytes, splenocytes and draining lymph nodes. Tumor growth was strongly inhibited in mice that exhibited efficient DC migration after RFA and OK-432-stimulated DC transfer, as compared to mice treated with RFA alone or treatment involving immature DC transfer. We also demonstrated that the antitumor effect of this treatment depended on both CD8-positive and CD4-positive cells. On the basis of our findings, we believe that combination therapy for metastatic liver cancer consisting of OK-432-stimulated DCs in combination with RFA can proceed to clinical trials, and it is anticipated to be markedly superior to RFA single therapy.

Keywords Metastatic liver cancer · MC38 · Immunotherapy · Intratumoral injection · Tumor-infiltrating lymphocyte

Abbreviations

RFA	Radiofrequency ablation
DC	Dendritic cell
HCC	Hepatocellular carcinoma
TAE	Transcatheter hepatic arterial embolization
TLR	Toll-like receptor
GFP	Green fluorescent protein
ELISPOT	Enzyme-linked immunospot
Treg	Regulatory T cell
MDSC	Myeloid-derived suppressor cell
IFN-γ	Interferon-γ

Introduction

Liver is one of the most common organs to which various cancers spread from their site of origin. In some types of cancer, the liver metastasis lesion is a target of surgical treatment. For instance, surgical resection of hepatic metastasis achieves longer median survival in colorectal and breast cancer patients [1, 2]. However, even if the hepatic lesions are surgically treated, the prognosis of the

Electronic supplementary material The online version of this article (doi:10.1007/s00262-013-1514-7) contains supplementary material, which is available to authorized users.

H. Nakagawa · E. Mizukoshi · N. Iida · T. Terashima · M. Kitahara · Y. Marukawa · K. Kitamura · S. Kaneko (✉)
Disease Control and Homeostasis, Graduate School of Medical Sciences, Kanazawa University, 13-1 Takara-machi, Kanazawa, Ishikawa 920-8641, Japan
e-mail: skaneko@m-kanazawa.jp

H. Nakagawa
e-mail: hidetoshi.naka@gmail.com

Y. Nakamoto
Second Department of Internal Medicine, Faculty of Medical Sciences, University of Fukui, Fukui 910-1193, Japan

K. Hiroishi · M. Imawari
Shin-yurigaoka General Hospital, Kawasaki, Kanagawa 215-0026, Japan

Published online: 03 January 2014

patients is not satisfactory. As for colorectal cancers, the recurrence rate is over 50 % after radical resection of metastatic lesions [3]. Moreover, at the time of initial diagnosis, only a few patients meet the criteria for hepatic resection because of unresectability, low hepatic functional reserve or poor performance status [4].

Radiofrequency ablation therapy (RFA) has been developed as a radical and minimally invasive treatment method for metastatic liver cancers. Recently, RFA has been used as an adjunct to hepatic resection or as an alternative method to resection when surgical treatment is not feasible [5]. Additionally, it has been revealed that RFA for metastatic liver cancers generates tumor antigen-specific T-cell responses in man [6, 7]. We have previously reported that RFA could also control distant tumor growth in a murine hepatocellular carcinoma (HCC) model [8].

Dendritic cells (DCs) are potent antigen-presenting cells [9]. Recently, we have established new treatments using local DC injection with transcatheter hepatic arterial embolization (TAE) and have shown that this combination therapy could induce tumor antigen-specific T-cell responses in HCC patients [10].

OK-432 is derived from the Su strain of Group A *Streptococcus pyogenes* by means of treatment with benzylpenicillin and heat [11]. OK-432 can stimulate DCs via Toll-like receptor (TLR) 3, TLR4 and β2 integrin and subsequently induce antigen-specific cytotoxic lymphocytes [12–14].

On the basis of these results, we hypothesized that OK-432-stimulated DC transfer is a promising candidate for an enhancer that can strongly increase the antitumor effect of RFA. We have previously demonstrated in a clinical trial that the local infusion of OK-432-stimulated DC after TAE could prolong recurrence-free survival in HCC patients [15]. However, it remains unknown as to how the transferred DCs work in combination with RFA. In the present study, we examined the antitumor effects of OK-432-stimulated DCs when combined with RFA and analyzed the functional mechanisms involved using a murine subcutaneous colon cancer model.

Materials and methods

Animals

Wild-type 8–12-week-old female C57BL/6 J mice were obtained from Charles River Japan (Yokohama, Japan). Female C57BL/6-Tg (UBC-GFP) 30Scha/J mice were purchased from the Jackson Laboratory (Bar Harbor, ME, USA). All animal experiments were approved and performed in accordance with the Guidelines for the Care and Use of Laboratory Animals of Kanazawa University, which strictly conforms to the Guide for the Care and Use of Laboratory Animals published by the US National Institutes of Health.

Cell lines and bone marrow-derived dendritic cells

A murine colorectal cancer cell line, MC38 and hybridomas, clone GK1.5 and clone 2.43 were cultured in RPMI-1640 containing 10 % fetal bovine serum (Life Technologies, Co., Carlsbad, CA, USA) supplemented with 100 μg/ml streptomycin and 100 units/ml penicillin (Wako Pure Chemical Industries Ltd., Osaka, Japan). Bone marrow-derived dendritic cells (BMDCs) were generated using 20 ng/ml of recombinant granulocyte macrophage colony-stimulating factor (R&D Systems, Minneapolis, MN, USA) as previously described [16]. OK-432 (Picibanil; Chugai Pharmaceutical Co. Ltd., Tokyo, Japan) was loaded into the supernatant from days 6–7 of the BMDC generation period at a concentration of 5 μg/ml.

In vitro evaluation of phagocytic activity by dendritic cells

MC38 cells were labeled with DiD dye (Life Technologies) according to the manufacturer's instructions followed by heat treatment at 80 °C for 90 s. OK-432-stimulated or immature DCs were co-incubated with the treated MC38 cells for 3 h at a ratio of 1:1. After incubation, the cell suspensions were observed using a fluorescence microscope (BZ9000: Keyence, Osaka, Japan) and analyzed by means of FACSCalibur (BD Immuno-Cytometry System, San Jose, CA, USA).

Animal model

Bilateral flanks of C57BL/6 mice were each injected subcutaneously with 1×10^6 MC38 cells. Seven days after injection, after they had grown to 5–6 mm in diameter, the subcutaneous tumors on one flank were treated using RFA, and 1×10^7 immature DCs or 1×10^7 OK-432-stimulated DCs were injected into the treated tumors at 24 h after RFA. After this, the volume of the untreated tumor on the contralateral flank was evaluated over a period of 10 days. Tumor volumes were calculated using the following formula: tumor volume (mm^3) = (longest diameter) × (shortest diameter)^2/2.

Radiofrequency ablation

Mice bearing tumors were anesthetized with an intraperitoneal injection of pentobarbital (Kyoritsu Seiyaku, Tokyo, Japan), and the skin on the tumor was cut. Subsequently, an expandable RFA needle was inserted into the tumor, which was treated using a radiofrequency generator (RITA

500PA; RITA Medical Systems, Inc., Fremont, CA, USA). During the use of this system, the intratumor temperature was maintained at 70–90 °C, and the current was turned off when the tumor exhibited heat denaturation.

Flow cytometry

The DCs were detected by means of staining with anti-CD11c antibodies (Life technologies). The lymphocytes in the draining lymph node were stained with anti-CD4 antibodies, anti-CD8 antibodies, anti-CD11c antibodies and anti-CD69 antibodies (BD Bioscience, San Diego, CA, USA). The splenocytes were stained with anti-CD4 antibodies, anti-CD8 antibodies, CD11c antibodies, anti-NK1.1 antibodies, CD45 antibodies (BD Bioscience), anti-Gr-1 antibodies, and anti-CD11b antibodies and mouse regulatory T-cell staining solution (BioLegend, San Diego, CA, USA). The stained samples were analyzed using FACSAria II (BD Immuno-Cytometry System).

Immunohistochemical assay

The draining lymph nodes and the observed tumors were embedded in Sakura Tissue-Tek optimum cutting temperature compound (Sakura Finetek Japan Co., Ltd., Tokyo, Japan) for frozen sectioning. Tissue sections were fixed at −20 °C in methanol for 10 min. The draining lymph nodes were stained using rabbit anti-GFP antibody (Abcam, Cambridge, UK) that were detected using an EnVision+/HRP kit (Dako, Glostrup, Denmark). The observed tumors were stained with anti-CD4 and anti-CD8a (BD Bioscience), which were detected using the Nichirei Histofine Simple Stain Mouse Max PO (Rat) system (Nichirei Co., Tokyo, Japan) or the Vectastain ABC kit (Vector Laboratory, Inc., Burlingame, CA, USA).

Interferon gamma enzyme-linked immunospot assay

The splenocytes, the tumor-infiltrating lymphocytes (TILs) in the untreated tumors that were isolated by mechanical homogenizations and density gradient centrifugations, and the lymphocytes in the draining lymph nodes were loaded into the interferon gamma enzyme-linked immunospot assay to estimate the tumor-specific immune reactions, as previously described [8, 17]. Briefly, 3×10^5 lymphocytes or 1×10^5 TILs were incubated for 24 h with or without 6×10^5 MC38 lysates, which were prepared through five cycles of rapid freezing in liquid nitrogen, thawing at 55 °C and centrifugation. The number of MC38-specific IFN-γ spots was determined by subtracting the number of spots incubated without MC38 lysates from the number of spots incubated with MC38 lysates. For CD4 or CD8 depletion, we used magnetic CD4 beads or CD8 beads (Miltenyi Biotec, Bergisch Gladbach, Germany).

In vivo CD4/CD8 depletion

For in vivo CD4 or CD8 depletion, B6 mice were injected intraperitoneally with 200 μg of purified monoclonal antibodies specific to CD4 or CD8 at 1 day before and 3 days after RFA treatment; the monoclonal antibodies were prepared from GK1.5 hybridoma and 2.43 hybridoma, respectively [18]. The depletion was confirmed by flow cytometry using peripheral blood lymphocytes stained with anti-CD4 and anti-CD8 antibodies.

Statistical analysis

The data obtained were analyzed statistically using the t test or one-way analysis of variance followed by Tukey's multiple-comparison test. A P value <0.05 was considered as being statistically significant.

Results

Migration efficacy and phagocytic ability of OK-432-stimulated DCs

We employed OK-432 as a modifying agent for DCs, because we have previously shown in clinical studies that OK-432 prolonged recurrence-free survival after combination therapy involving DC injection with TAE for HCC patients [10, 15]. We first confirmed that the OK-432-stimulated murine DCs showed higher expression of maturation markers such as CD40, CD80, CD86, MHC class II and CCR7 (Supplementary Fig. 1), as previously reported [19, 20].

To evaluate their phagocytic abilities, we incubated the immature DCs and the OK-432-stimulated DCs with MC38 tumor cells. Heat-treated MC38 cells were taken up well by both immature DCs and OK-432-stimulated DCs, as compared to nontreated MC38 cells (Fig. 1a–c). In addition, the phagocytic ability of OK-432-stimulated DCs was not inferior to that of immature DCs. These results were consistent with the dextran uptake assay (Supplementary Fig. 2) and our previous data on human monocyte-derived DCs [15]. Since heat-treated MC38 cells were thought to be in a similar condition to those in the MC38 tumor in mice treated with RFA, OK-432-stimulated DCs were expected to effectively phagocytose RFA-treated MC38 tumor cells in vivo.

We next estimated the kinetics of the transferred DCs in mice bearing subcutaneous MC38 tumors treated with RFA. Immature DCs or OK-432-stimulated DCs that were derived from GFP-Tg mice were injected intratumorally

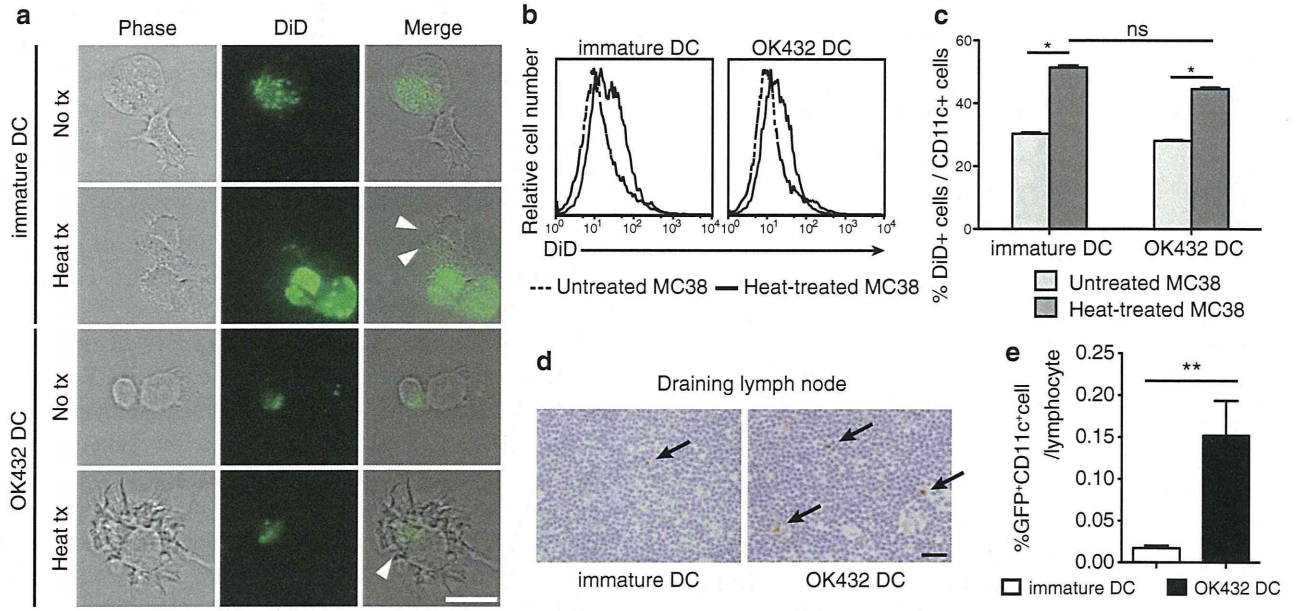

Fig. 1 Effects of OK-432 on murine bone marrow-derived DCs. **a** OK-432-stimulated DCs or immature DCs were co-incubated for 3 h with MC38 cells untreated or treated at 80 °C for 90 s after staining with DiD dye. After incubation, DC and MC38 cells were observed using a fluorescence microscope. *Arrowheads* indicate MC38 derivatives being phagocytosed by DCs. No tx, untreated MC38 cells; heat tx, heat-treated MC38 cells; *bar*, 20 μm. **b**, **c** Co-incubated MC38 cells and DCs were stained with anti-CD11c antibodies and analyzed using flow cytometry. The *histograms* show the DiD fluorescent intensity of the CD11c-positive fractions. The percentages of DiD^+ $CD11c^+$ cells in the $CD11c^+$ cell population are also shown in a *column graph*. The experiments were performed five times, and representative results are shown. Data are presented as the mean ± SE. $*P < 0.05$. **d** The migration abilities of the DCs after intratumoral transfer were evaluated. The draining lymph nodes were harvested at 3 days after RFA followed by the DC transfer. Frozen sections were prepared and stained with anti-GFP antibodies. *Arrows* indicate the GFP-positive cells in the lymph nodes. *Bar* 20 μm. **e** The draining lymph nodes were also analyzed using flow cytometry after staining with anti-CD11c antibodies. Data were obtained from six mice in each group. Percentages of GFP^+ $CD11c^+$ cell are presented as the mean ± SE. $**P < 0.01$

at 24 h after RFA treatment, and the subcutaneous tumors and the lymph nodes were harvested at 3 days after RFA. According to the immunohistochemical study involving the detection of GFP, the inguinal lymph node on the RFA-treated flank was thought to be the draining lymph node (Supplementary Fig. 3). Additionally, the number of transferred DCs in the draining lymph nodes was significantly higher in the mice treated with the OK-432-stimulated DCs than in those treated with the immature DCs (Fig. 1d, e). Our experimental results attested to the fact that the OK-432-stimulated DCs had both sufficient phagocytic ability and higher migration efficacy.

Effect of RFA in combination with the injection of OK-432-stimulated DCs on tumor growth

OK-432-stimulated DCs were used in combination therapy with RFA in this murine model (Fig. 2a). Namely, BMDCs stimulated with OK-432 were injected into RFA-treated tumor at 24 h after RFA treatment. We compared four groups of tumor-bearing mice as follows: (1) no treatment; (2) RFA only; (3) RFA with the injection of immature DCs; and (4) RFA with the injection of OK-432-stimulated DCs. Tumor volumes were measured for 10 days after treatment/no treatment. On the day after RFA, the treated tumors were covered with scars, started to shrink and had disappeared macroscopically at 4 days after RFA in all of the groups. This indicated that RFA treatment was highly effective for focal lesions. The injected DCs were detected in the treated tumors (Supplementary Fig. 3). With regard to the untreated tumors, as we previously reported, the group treated with RFA only showed an antitumor effect against distant tumors. The injection of immature DCs combined with RFA did not show any additional enhancement of the antitumor effect. On the other hand, the volumes of the untreated tumors in the group that underwent RFA combined with the injection of OK-432-stimulated DCs were strongly suppressed ($P < 0.001$) relative to other groups (Fig. 2b).

Recruitment of antigen-specific lymphocyte fractions in both splenocytes and tumor by injected OK-432-stimulated DCs

Ten days after RFA, the tumors and the spleens were harvested and analyzed using immunohistochemical staining.

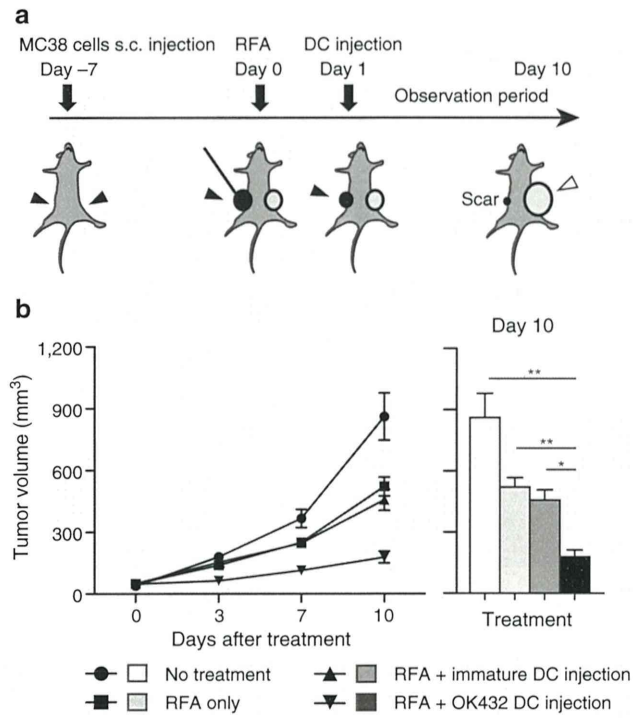

Fig. 2 Impact of injection of OK-432-stimulated DCs into murine MC38 subcutaneous tumors. **a** RFA was administered to a tumor on one flank followed by injection of 1×10^7 DCs into the treated tumor. The untreated tumor on the opposite flank was observed for 10 days. The *solid arrowheads* indicate the treatment intervention sites, and the *open arrowhead* indicates the observed untreated tumor. **b** The tumor volumes were compared among the four groups as follows: (1) no treatment; (2) RFA only; (3) RFA in combination with immature DC injection; and (4) RFA in combination with OK-432-stimulated DC injection. $n = 8$ mice per group. The data are presented as the mean ± SE. $^*P < 0.05$; $^{**}P < 0.001$

We examined the number of tumor-infiltrating CD4-positive or CD8-positive cells in the tumors by means of immunohistochemistry. The infiltration of these cells into the untreated tumors was found to be promoted by RFA. The injection of OK-432-stimulated DCs after RFA induced the additional recruitment of CD8-positive cells into the untreated tumors (Fig. 3a, b). CD11c-, CD11b- and NK1.1-positive cells were very marginal and showed no differences in number among the four groups (data not shown).

Systemically, in terms of analyzing splenocytes with flow cytometry, the number of CD4-positive and CD8-positive cells increased in the group treated with RFA in combination with OK-432-stimulated DCs. On the other hand, the CD11c and NK1.1 fractions, which were considered as DCs and NK cells, respectively, presented no difference among the four groups (Fig. 3c). In addition, we examined the effect of the injection of OK-432-stimulated DCs after RFA on inhibitory blood cells such as regulatory T cells (Tregs) and myeloid-derived suppressor cells (MDSCs) (Fig. 3c). Among CD4-positive cells, significantly fewer Tregs were detected in the group treated with RFA in combination with OK-432-stimulated DCs than in the group treated with RFA in combination with immature DCs. In the analysis of MDSCs, their rates of occurrence were not affected by treatment with either RFA alone or RFA in combination with DCs. Taking these results together, we concluded that treatment with RFA combined with OK-432-stimulated DCs enhanced the number of CD4- or CD8-positive T cells and reduced the Treg/CD4 ratio, but did not influence MDSC numbers.

Furthermore, we examined the number of tumor-specific IFN-γ-producing cells at 10 days after RFA using the ELISPOT assay. The number of IFN-γ-producing cells among splenocytes and TILs showed the same trend as the level of tumor growth control among the four groups (Fig. 3d); the group treated with RFA in combination with injected OK-432 DCs showed the most abundant specific spots. These results suggested that the augmented antitumor effects of RFA combined with OK-432-stimulated DCs depended in large part on tumor-specific immune responses by CD4 cells or CD8 cells.

Evaluation of tumor-specific immune responses in the draining lymph node after OK-432-stimulated DC transfer

CD4 T cells and CD8 T cells are now thought to have an important antitumor effect as a result of the OK-432-stimulated DC transfer. To elucidate the priming of the antigen-specific immune response, we analyzed the draining lymph nodes at 3 days after RFA focusing on CD4-positive or CD8-positive cells. CD69, the early activation marker, on CD4-positive and CD8-positive cells was examined and compared between the immature DC transfer group and the OK-432-stimulated DC transfer group. It was found that CD69 expression on both CD4-positive and CD8-positive cells was elevated in the OK-432-stimulated DC transfer group (Fig. 4a, b). The activations were also demonstrated to be tumor-specific using the IFN-γ ELISPOT assay in which each of CD4-negative and CD8-negative fractions was applied to the assay and both showed tumor-specific IFN-γ secretions (Fig. 4c).

Evaluation of the relationship between CD4-positive and CD8-positive cells and the antitumor effects of RFA and OK-432-stimulated DC transfer

We have demonstrated that combination therapy involving RFA and OK-432-stimulated DC transfer might generate enhanced antitumor effects via tumor-specific CD4-positive and CD8-positive cells. To obtain further evidence, we carried out in vivo CD4 or CD8 depletion studies in mice. Initially, we confirmed CD4 or CD8 depletion in the control in vivo study (Supplementary Fig. 4). The

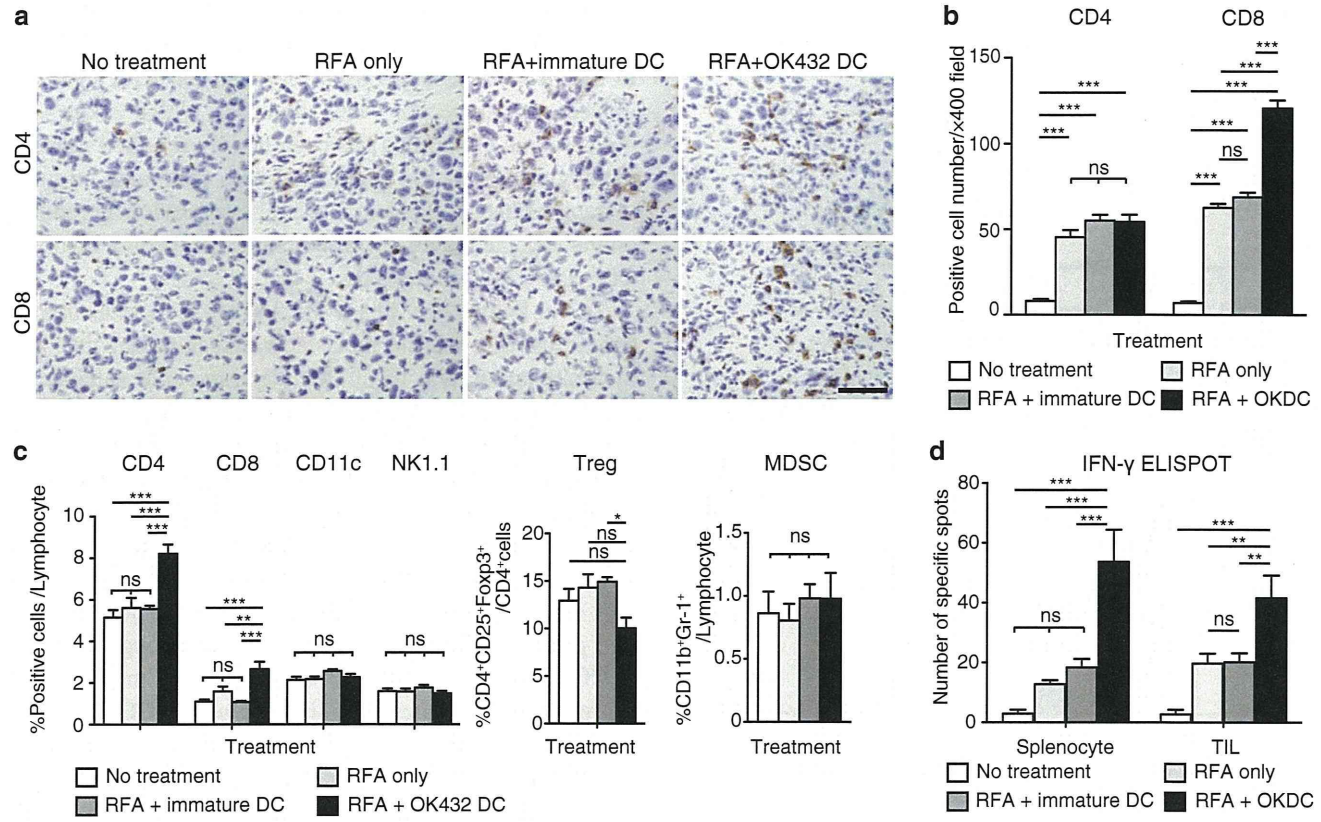

Fig. 3 Analysis of the tumor-infiltrating lymphocytes and the splenocytes after combination therapy with RFA and DC injection. **a** CD4-positive and CD8-positive cells in the observed untreated tumors were detected using immunohistochemistry at 10 days after RFA. The *black bar* represents 50 μm. **b** The number of positive cells was counted using a microscope. This was achieved by counting the number of cells in six randomly chosen tumor areas at 400-fold magnification. Three mice were used in each group. The data are presented as the mean ± SE. *** $P < 0.001$; *ns* not significant. **c** Ten days after RFA, splenocytes were stained with anti-CD4, anti-CD8, anti-NK1.1 and anti-CD11c antibodies and analyzed using flow cytometry. Regulatory T cells (Tregs) defined as $CD4^+CD25^+Foxp3^+$ cells and myeloid-derived suppressor cells (MDSCs) defined as $CD11b^+Gr\text{-}1^+$ cells were counted and compared among the four groups. Six mice were analyzed in each group. The data are presented as the mean ± SE. *$P < 0.05$; **$P < 0.01$; ***$P < 0.001$; *ns* not significant. **d** Immune responses by the splenocytes and the tumor-infiltrating lymphocytes (TILs) were examined by means of the IFN-γ enzyme-linked immunospot (ELISPOT) assay using MC38 lysate. In the assay for TILs, 1×10^5 TILs were mixed with 2×10^5 splenocytes from B6 mice and applied to the well. Six mice were analyzed in each group. The data are presented as the mean ± SE. **$P < 0.01$; ***$P < 0.001$; *ns* not significant

CD4-positive and CD8-positive fractions in the peripheral blood were greatly depleted at 7 days after injection of the antibodies. The experimental schedule was determined as follows. The depletion antibodies were injected at 1 day before and 3 days after RFA, and the tumors that were not treated with RFA were observed for 10 days. In addition, the draining lymph nodes were harvested at 3 days after RFA and analyzed (Supplementary Fig. 5). The antitumor effects of RFA treatment and the augmented effects from OK-432-stimulated DCs were cancelled out by depletion of both CD4 and CD8 cells (Fig. 5a). In the CD4 depletion study, there was no priming of the antitumor effect in the draining lymph nodes (Fig. 5b; Supplementary Fig. 6). On the other hand, in the CD8 depletion study CD4 cells were activated with tumor specificities in the draining lymph node in both groups, and the activation was stronger in the OK-432-stimulated DC transfer group (Fig. 5b; Supplementary Fig. 6). Tumor-specific reactions were also demonstrated in the splenocytes and the TILs at 10 days after RFA. There was a tendency for OK-432 DC transfer treatment to result in the recruitment of increased numbers of tumor-specific lymphocytes into the tumor on the opposite flank ($P = 0.184$; Fig. 5c). These results indicated that the tumor-specific activation of CD8 cells was necessary for the antitumor effect and was completely dependent on help from the CD4 cells.

Discussion

In the past decade, cytotoxic agents and molecular-targeted therapies have been developed, and the treatment outcomes

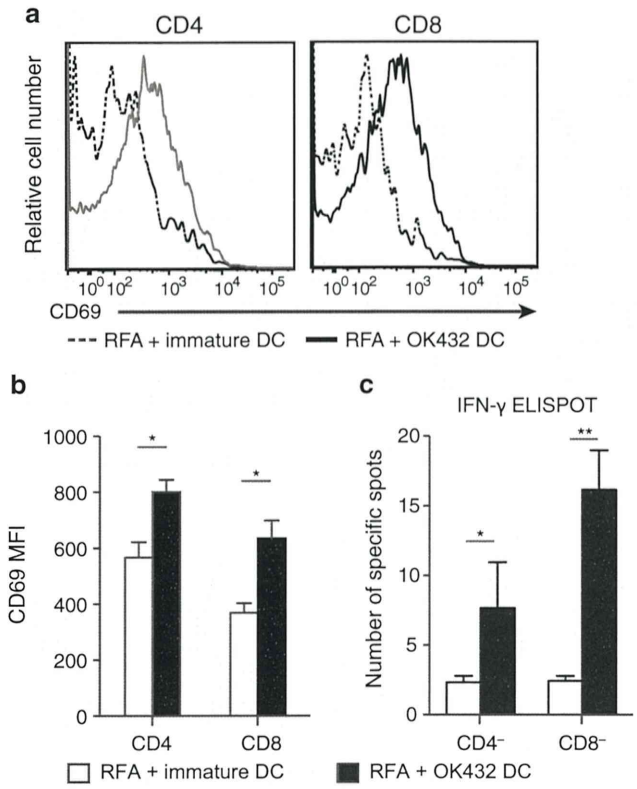

Fig. 4 Antigen-specific activation of both CD4-positive and CD8-positive cells in the draining lymph node. **a** Three days after RFA followed by DC transfer, the draining lymph node was harvested and analyzed by staining with anti-CD4 antibodies, anti-CD8 antibodies and anti-CD69 antibodies. The fluorescence intensities of CD69 in the CD4-positive and CD8-positive fractions are compared between the OK-432-stimulated DC transfer group and the immature DC transfer group. The data were obtained from six mice in each group. The *histograms* show the representative data. **b** The mean fluorescent intensities are also presented as the mean ± SE. $*P < 0.05$. **c** The antigen specificities of the T-cell activations were confirmed by means of the IFN-γ ELISPOT assay using MC38 lysate. After CD4 or CD8 depletion using CD4 and CD8 magnetic beads, the lymphocytes from the draining lymph nodes were submitted to IFN-γ ELISPOT assay. Data were obtained from six mice in each group. $*P < 0.05$; $**P < 0.01$

for various cancers have improved. However, few patients with advanced cancers have been completely cured, and thus, new strategies for anticancer therapy are required. Immunotherapy is considered to have the potential to effectively treat such advanced cancers, and many different approaches have been explored. For the utilization of the adoptive immune response in a cancer therapy, DCs are a key constituent of the immune system. This is because of their natural potential to present tumor-associated antigens to $CD4^+$ and $CD8^+$ lymphocytes and also to control both immune tolerance and immunity [21]. Thus, DCs are considered as an important target for cancer immunotherapy. Many trials and studies have been carried out regarding immunotherapy for cancer using DCs, some of which have been reported to have pronounced effects [22–25]. In recent studies, it has been revealed that RFA treatment induces tumor-specific T-cell responses, which is known as the abscopal effect; this has been mainly reported in radiotherapy studies and is augmented with combined immunotherapies [26, 27]. Brok et al. [28] have previously reported on the vaccination effects of combination therapy involving RFA and CTLA-4 antibody.

To our knowledge, this is the first study that has demonstrated using a murine metastatic cancer model that RFA in combination with focal DC injection could enhance the antitumor effects of RFA alone. Our results showed that immature DCs made no additional immunological contribution to RFA. In the analysis of draining lymph nodes, few transferred DCs were detected after the injection of immature DCs. It appeared that immature DCs did not act as sentinels in the adoptive immune system, partially because they exhibited low expression of CCR7 (the main molecule that promotes DC migration [29]), even though elevation of CCR7 expression using OK-432 was very modest in our study. There is another possibility immature DCs are easily lysed and excluded by the host immune system [30]. On the other hand, mature DCs can escape cell lysis [31].

Utilization of OK-432-stimulated DCs improved the number of migrating transferred DCs in the present study. These DCs, which could act as sentinels for immunity, induced expansion in the number of tumor-specific lymphocytes in the draining lymph nodes, in the splenocytes and in the distant nontreated tumors, without systemic expansion of inhibitory cells such as Tregs or MDSCs. We also demonstrated that these augmented antitumor effects after OK-432-stimulated DC transfer were primed in the draining lymph nodes with tumor-specific activations of CD4-positive and CD8-positive cells; it was proved that without CD4-positive or CD8-positive cells, both the antitumor effect by RFA and the additional effect of the injection of OK-432-stimulated DCs disappeared completely. In addition, the in vivo CD4 depletion study revealed that tumor-specific activations of CD8-positive cells were not seen in the draining lymph nodes in both groups after the injection of immature DCs and OK-432-stimulated DC injection; in other words, tumor-specific CD8 activation depended on CD4-positive cells entirely. In the CD8 depletion study, on the other hand, we found that tumor-specific CD4-positive cells appeared in the draining lymph nodes, the splenocyte population and the untreated tumor on the opposite flank, and these lymphocytes were considered to be CD4-positive cells. In the tumor-infiltrating lymphocytes, there was a tendency for more tumor-specific CD4-positive cells to be recruited after treatment involving OK-432-stimulated DC transfer. Many researchers have demonstrated the contribution of CD4 cells to cytotoxicity